JHT Mid-term Report
August 1, 2010 – March 31, 2011

Improvement in the rapid intensity index by incorporation of inner-core information

Principle Investigator: John Kaplan
Hurricane Research Division
NOAA/AOML

Co-PIs: Mark DeMaria NOAA/NESDIS, Joe Cione (NOAA/HRD), John Kaff (NOAA/NESDIS), Jason Dunion (CIMAS/HRD, John Dostalek (CIRA), Jun Zhang (CIMAS/HRD)

Co-Investigators: Thomas Lee (NRL), Jeffrey Hawkins (NRL)

Scientific/Computer scientist support: Evan Kalina (CU), Paul Leighton NOAA/HRD

Accomplishments:

1. Operational RII verification

The current discriminant analysis version of the SHIPS Rapid Intensification Index (RII) has been used operationally at the National Hurricane Center since the start of the 2008 Hurricane season. Figure 1 shows the skill of the operational 2008-2010 RII forecasts for both the Atlantic and E. Pacific basins when the RII forecasts were assessed relative to climatology based upon a Brier skill score following the methodology of Kaplan et al. (2010). It can be seen that the RII forecasts were generally skillful (except for the 35-kt threshold in the Atlantic) in each basin. Interestingly, the skill of the RII is found to decrease as the RI threshold increases in the Atlantic basin while a trend of increasing skill with increasing RI threshold magnitude is found for the E. Pacific.

Although the aforementioned results indicate that the current operational RII did exhibit some skill for the period 2008-2010, the skill was still on the low side for this period underscoring the need for additional research to improve the RII. Thus, the motivation of this current JHT project has been to attempt to improve the existing operational RII by adding predictors derived from three new sources of information: total precipitable water (TPW) deduced from SSM/I and TRMM (and AMSU in the real time version of the RII) imagery, principle components derived from analysis of GOES-IR imagery and boundary-layer predictors deduced from low-level GFS temperature and moisture fields. A description of the newly derived experimental Atlantic and E. Pacific versions of the RII that were developed using these new data sources is provided below.

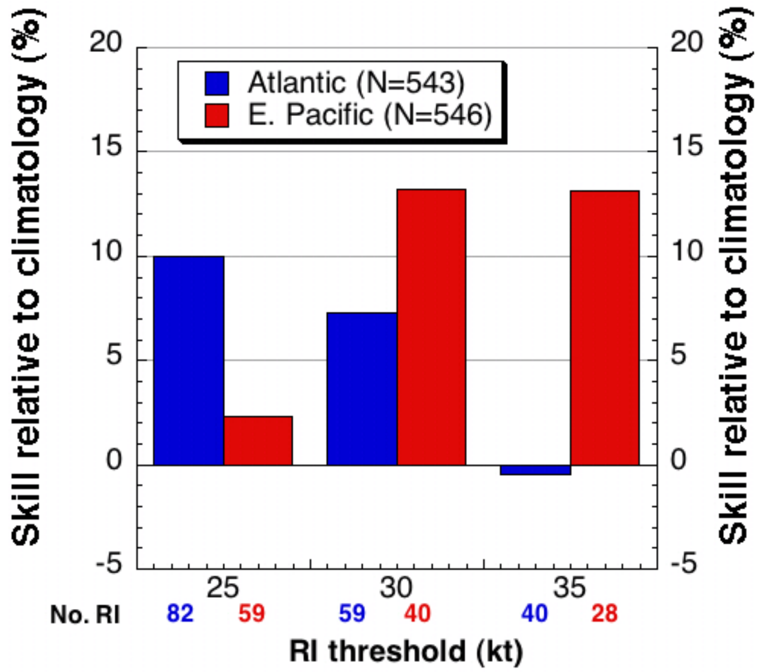

Fig. 1. The skill of the 2008-2010 operational RII forecasts. The number of RI cases for each RI threshold is also provided for both the Atlantic (blue) and E. Pacific (red) basins along the x-axis.

2. Derivation of Experimental RII

a. Atlantic Experimental RII

As a first step at screening predictors derived from the above three new sources for their ability to increase the skill of the operational RII, each was subjected to statistical significance testing for a homogenous sample of Atlantic cases for the 1995-2008 sample. Those predictors whose mean values for the developmental RI and non-RI samples were shown to be statistically different (at $\geq$ 99.9% level based upon a standard 2-sided t-test) were tested for their ability to increase the skill of the operational RII. This was accomplished by substituting the statistically significant predictors for similar predictors in the existing operational RII shown in Table 1. Specifically, the new TPW predictors were tested as replacement to the 850-700 mb relative humidity (RH) predictor since both are measures of atmospheric moisture, while the GOES-IR PC predictors were tested as replacement for the two existing inner-core GOES predictors since they are all measures of inner-core organization as deduced using GOES IR imagery. Finally, the new GFS boundary-layer predictors were tested as a replacement predictor to the potential intensity and ocean heat content predictors since each of these is related to boundary-layer processes.

Previous 12-h intensity change
850-200 mb vertical shear from 0-500 km radius (24-h mean)
200 mb divergence from 0-1000 km radius (24-h mean)
850-700 mb relative humidity from 200-800 km radius (24-h mean)
% area from 50-200 km covered by -30°C GOES-IR brightness temperatures at T=0 h
Std. dev of 50-200 km GOES-IR brightness temperatures at T= 0 h
Potential intensity (Current intensity – maximum potential intensity)
Oceanic heat content (24-h mean)

Table 1. Predictors used in the current operational Atlantic RII.

Sensitivity tests were then performed to determine if any of the new predictors increased the skill of the RII when they were substituted for the specified predictors described above that are currently included in the existing operational RII (see Table 1). The change in skill of each of the new predictors was then assessed by comparing the average skill of the experimental RII to that obtained using the current operational RII predictors for the three RI thresholds that are used in the current operational RII (25-kt, 30-kt, and 35-kt) as well as an additional RI threshold of 40-kt for which a version of the RII was developed and tested at the request of one of our NHC points of contact (Eric Blake) using the methodology described in Kaplan et al. (2010).

Based upon the above sensitivity tests, three new predictors were selected for use in the new experimental versions of the RII. The first of these predictors is the percentage of the area within 500 km radius 90° up-shear of the storm center with TPW < 45 mm at time t=0 h. This predictor is used as a replacement to the 850-700 mb RH in the new experimental version of the Atlantic RII. Rapid intensification is favored when this predictor is small and hence the amount of low to mid-level dry air that is being advected into the storm circulation is relatively small. The cutoff of 45 mm as a delineator for low to mid-level dry air is based upon the results of Dunion (2011). Figure 1 shows an example of the distribution of TPW on a select day during the 2003 Hurricane season. The blue and green areas (TPW <45 mm) represent regions where the atmosphere is relatively dry between the surface and 500 mb (where 90-95% of the contribution from TPW comes from) while the orange and red areas (TPW > 45 mm) represent regions where the atmosphere is relatively moist.

Total Precipitable Water (TPW) RII Predictor

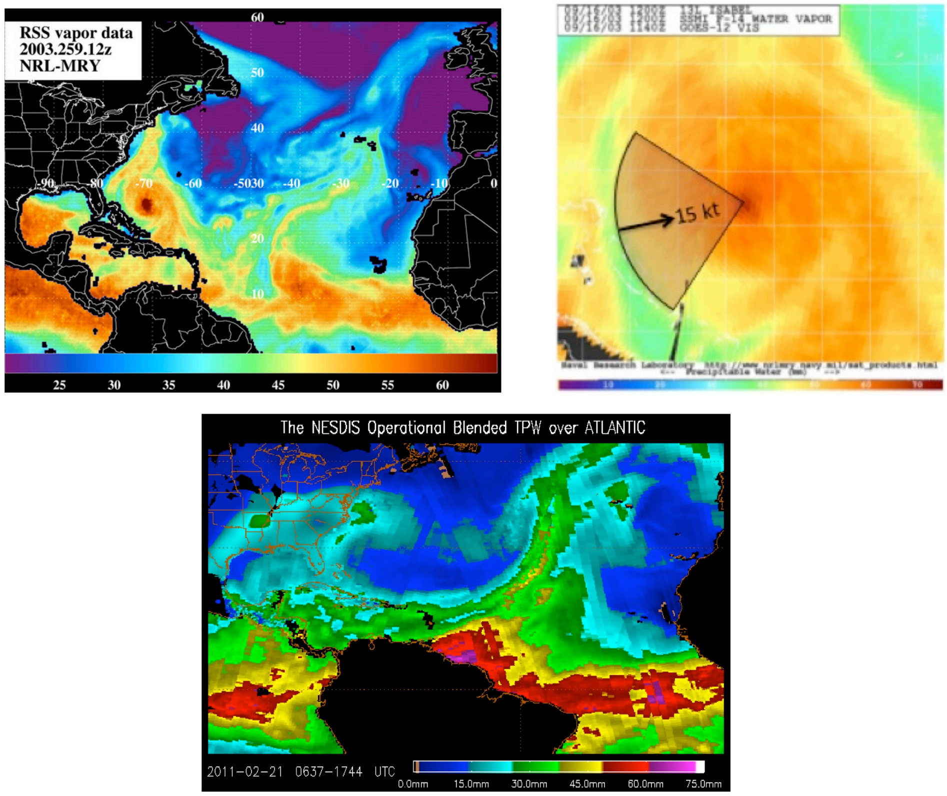

Fig. 2. Total precipitable water (TPW) for a select day and time (9/16 at 12 UTC) during the 2003 Hurricane Season (top left panel). A close-up view showing the area over which the TPW predictor is computed is also depicted for Hurricane Isabel located several hundred kilometers east of Florida at this time (top right panel). An example of the blended NESDIS operational TPW analysis from 21 February 2011 is also provided (bottom panel).

The second new RI predictor is the second principle component (PC2) computed from the GOES-IR imagery following the methods described in Knaff (2008). This predictor is used as a replacement for the percent area covered with GOES-IR brightness temperatures <-30° C in the new experimental version of the Atlantic RII. Figure 3 shows the favored overall pattern of the EOF for PC2 as well as an example of what the GOES-IR imagery looked like just prior to Hurricane Wilma's period of RI during the 2005 Hurricane Season. The image indicates that convection tends to be enhanced in the left front quadrant (along the direction of motion) while being suppressed in the right rear quadrant near the time that RI commences which may be an indication that the environment ahead of the storm is relatively conductive for convection. Knaff (2008) found that the aforementioned pattern often precedes axisymmetrizaton of the IR imagery deduced convection. It should be noted, however, that a more symmetric overall inner-core GOES-IR signature has been previously determined to be favored for RI (Kaplan et al. 2010). Thus, the above results indicate that if any asymmetries in the convective field do exist (which they typically do) then a pattern of enhanced (suppressed) convection in the left front (right rear) quadrant along the direction of motion is most conducive for RI.

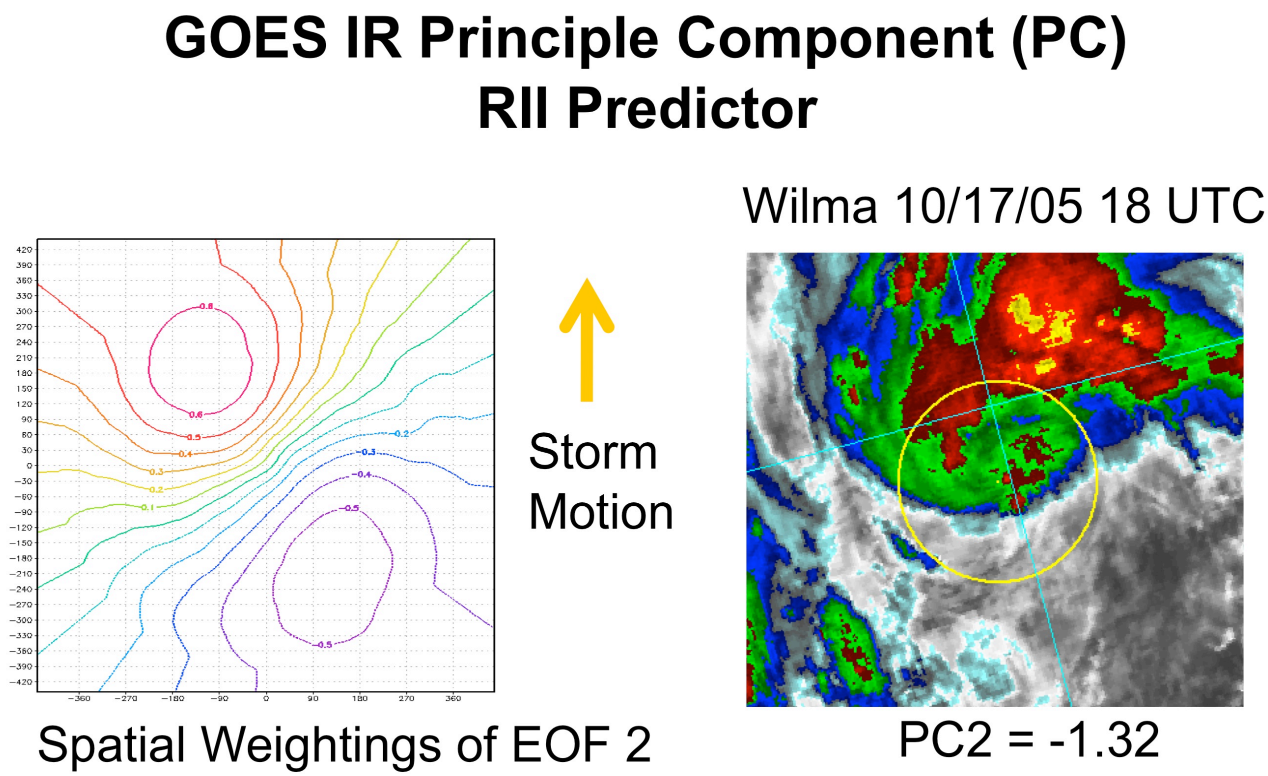

Fig. 3. Preferred pattern of PC2 (left) and an example of the corresponding GOES-IR representation for Hurricane Wilma at 18 UTC on 17 October 2005 (right). The yellow circle denotes a circle with a radius of 440 km over which the PCs were evaluated. The direction of motion is to the top center of both diagrams.

The last new predictor is the inner-core dry air parameter that is given by:

$$(q10_{layer} - q10)*Vmx \quad (1)$$

where q10 is the inner-core specific humidity at 10 m obtained using the GFS 1000 mb temperature and relative humidity (RH) between 200 and 800 km radius, $q10_{layer}$ is the 10 m specific humidity obtained using the ambient 200-800 km radius 1000 mb T and the layer-mean RH from 1000 mb to 500 mb, and Vmx is the NHC maximum sustained wind at t=0 h. The value of q10 is obtained by bringing the 1000 mb air down to the surface (dry adiabatically if unsaturated at 1000 mb and moist adiabatically if air is saturated) and then allowing the air to cool assuming that the RH reaches 95% as the parcel spirals into the storm core (Cione and Uhlhorn 2003). The value of $q10_{layer}$ is obtained following the same methodology using the 1000 mb T but using the layer-mean RH between 1000 and 500 mb instead of using only the RH at 1000 mb. It should be noted that small values of the inner-core dry air parameter, indicating less potential for dry air to mix down to the surface, are favored for RI. Although initial testing of this predictor as a replacement for potential intensity and/or ocean heat content on cases from the 1995-2008 database showed that it increased the skill of the RII when used in place of ocean heat content, additional testing conducted after cases from the 2009 Hurricane Season were added to the existing database showed that the skill of the RII was maximized when all three (ocean heat content, inner-core dry air predictor, and potential intensity) were used as RII predictors. Thus, the new experimental version of the Atlantic RII has a total of 9 predictors as is shown in Table 2.

Finally, in addition to utilizing three new RI predictors, the scaling methodology that was used for the potential intensity and persistence predictors was modified slightly since sensitivity tests showed that doing so improved the overall skill of the model for the developmental sample. This new scaling technique was formulated so that the both the potential and persistence values were most favored for RI when they were equal to the mean value of each respective RI predictor for all of the RI cases in the developmental sample. Figure 4 shows that this new experimental RII yielded an increase in skill of anywhere from 2 – 6 % over the current operational version for the developmental sample with an average absolute skill improvement of 3 %(15% relative) observed for the four RI thresholds studied.

Previous 12-h intensity change
850-200 mb vertical shear from 0-500 km radius (24-h mean)
200 mb divergence from 0-1000 km radius (24-h mean)
Percent area with TPW < 45 mm within 500 km radius 90° upshear (T= 0 h value)
Second principle component of GOES-IR imagery within 440 km radius (T=0 h value)
Std. dev of 50-200 km GOES-IR brightness temperatures (T= 0 h value)
Potential intensity (Current intensity – maximum potential intensity)
Oceanic heat content (24-h mean)
Inner-core dry air parameter (24-h mean)

Table. 2 Predictors used in the Experimental Atlantic RII.

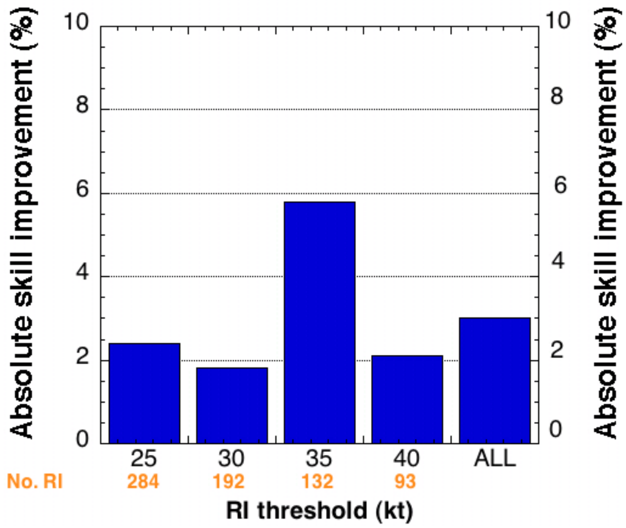

Fig. 4. Improvements of the new Atlantic Experimental RII over the current operational version for the 1995-2009 dependent sample (N=2524). The numbers of RI cases for each threshold are shown in orange along the x-axis.

b. E. Pacific Experimental RII

An E. Pacific version of the RII that included the same nine predictors that were used in the Atlantic experimental RII described above as well as one additional predictor (the initial NHC estimated maximum sustained wind) was derived using data for the period 1995-2009. A list of the predictors used in the new experimental E. Pacific RII is provided in Table 3. It should be noted that the new scaling methodology that was originally developed for use in the experimental version of the Atlantic RII degraded the E. Pacific version when tested on the developmental sample. Thus, when deriving the new experimental version of the E. Pacific RII, the persistence and potential predictors were treated using the same methodology that is used in the current operational RII. Results indicate that the new E. Pacific version of the RII exhibited mean absolute improvements ranging from 0.2-3.2% with an average absolute skill improvement of 2 % (10% relative improvement) over the current operational version for the 4 RI thresholds for the dependent sample studied.

Previous 12-h intensity change
850-200 mb vertical shear from 0-500 km radius (24-h mean)
200 mb divergence from 0-1000 km radius (24-h mean)
Percent area with TPW < 45 mm within 500 km radius 90° up-shear at T=0 h
Second principle component of GOES-IR imagery within 440 km radius at T= 0 h
Std. dev of 50-200 km GOES-IR brightness temperatures at T= 0 h
Potential intensity (Current intensity – maximum potential intensity)
Oceanic heat content (24-h mean)
Inner-core dry air predictor (24-h mean)
T=0 h maximum sustained wind

Table 3. Predictors used in the new experimental E. Pacific RII.

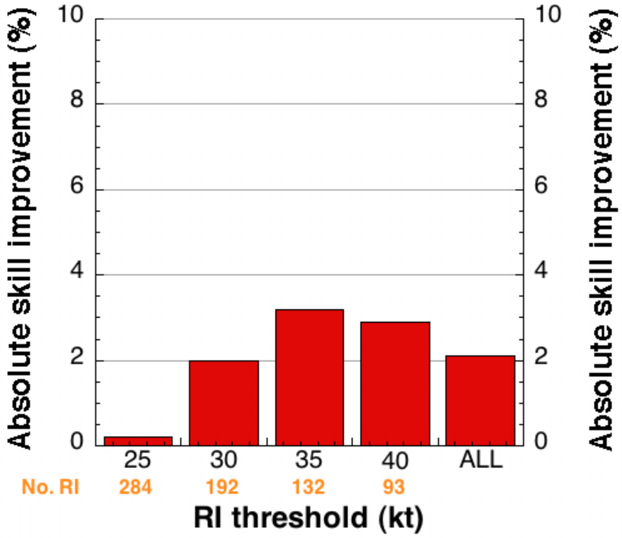

Fig. 5. Improvements of the new E. Pacific Experimental RII over the current operational version for the 1995-2009 dependent sample (N=2422). The numbers of RI cases for each RI threshold are depicted in orange along the x-axis.

3. Results

a. Atlantic Experimental RII Verification

Since the experimental version of the Atlantic RII was only first run in real-time and made available to forecasters at the NHC via a web site at CIRA in mid September of the 2010 Hurricane Season, it was re-run for all cases from 2008-2010 to provide a more representative assessment of its likely level of performance. To accomplish this, all of the forecast cases from 2008-2010 were re-run using the real-time GFS forecast fields and the NHC forecast tracks. Prior to performing the re-runs for a given year, both the operational and experimental versions of the RII were first re-derived by excluding all cases from that particularly year. Consequently, the skill shown below should closely mimic that which would have otherwise been obtained had these forecasts been made in real-time for this three-year period. It should be noted that the number of re-run forecasts is slightly lower than the number of operational forecasts since the data required to compute the PC predictor were not available for some forecasts made early in a storm's lifecycle particularly for cases prior to 2010 when this predictor was not routinely computed.

Figure 6 shows the skill of the Atlantic RII for the original experimental version of the RII (Experimental_V1) as well as for a second version of the RII that was derived using the same exact predictors and methods that were used to derive the E. Pacific version described above. This second version (Experimental_V2) was tested since it is desirable to have the same version of a model running in both basins and dependent tests showed that it was also superior to the version that had been previously developed for use in the Atlantic. It can be seen that the Experimental_V2 version of the new Atlantic Experimental RII was more skillful than the Experimental_V1 version for all 4 RI thresholds. It is also noteworthy that both versions of the new Atlantic Experimental RII performed better relative to the operational version for the lower RI thresholds (25-kt and 30-kt). This is particularly true for the Experimental_V2 version that was found to have skill that was 6.7 and 13 % greater than the operational version for the 25-kt and 30-kt RI thresholds, respectively. The performance of both the new Experimental and operational versions of the Atlantic RII was very similar for the highest 2 RI thresholds which differs from the dependent results shown above, which indicated that the largest improvements for the Experimental RII were found for the higher RI thresholds. Perhaps, the smaller number of RI cases that were available for both deriving and verifying the RII are responsible for the less impressive performance of the Experimental Atlantic RII at the higher RI thresholds. Alternatively, perhaps the degradation is due to a greater sensitivity to the use of real-time GFS forecast fields and NHC forecast tracks for the re-run forecasts made for the higher RI thresholds.

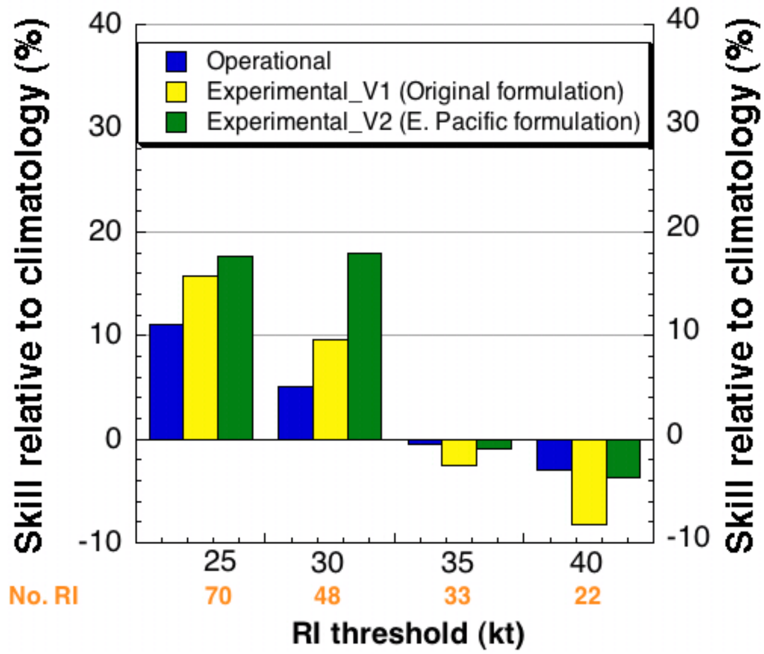

Fig. 6. Skill of the new Experimental Atlantic RII for the original formulation (Experimental_V1) and the newer version that uses the same predictors and methodology used to derive the new Experimental E. Pacific RII (Experimental_V2) for the 2008-2010 re-run forecasts (N=503). Also shown for comparison is the skill of the operational version of the RII for those same re-run forecasts. The numbers of RI cases for each RI threshold are provided in orange.

b. E. Pacific Experimental RII Verification

Figure 7 shows the skill of the E. Pacific 2008-2010 re-run forecasts that was obtained using the same verification methods that were used for the Atlantic basin. It can bee seen that the new experimental E. Pacific RII was generally more skillful than the current operational version for the lowest three RI thresholds (25-kt, 30-kt, and 35-kt) by 0.5 to 5.5 % but had less skill for the 40-kt RI threshold although both versions were still quite skillful for this threshold. It is interesting to note that in addition to exhibiting more skill than the Atlantic versions both the experimental and operational versions of the E. Pacific RII exhibited increasing skill with increasing RI threshold magnitude while Fig. 6 shows that the New Experimental versions of the Atlantic RII showed the opposite trend of decreasing skill with increasing RI threshold magnitude. These opposing trends in skill as a function of RI threshold for the Atlantic and E. Pacific basins were also found for the 2008-2010 operational RII forecasts (Fig. 1).

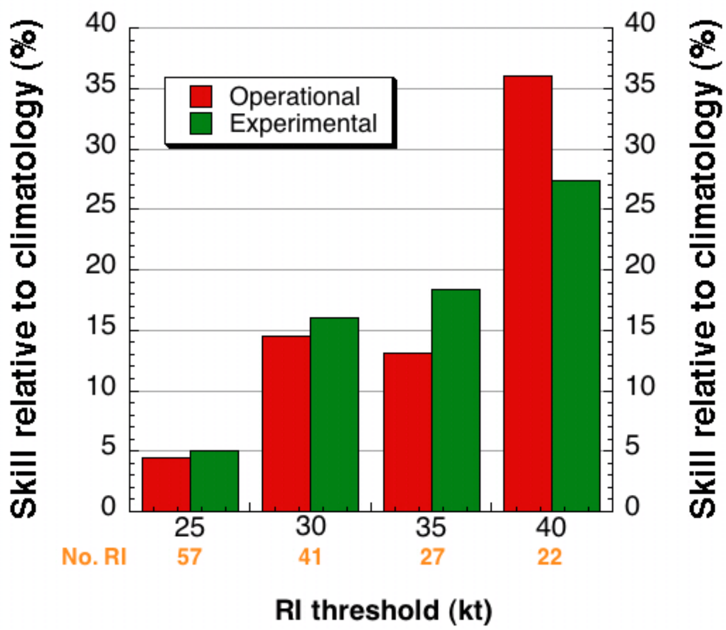

Fig. 7. Skill of the new Experimental E. Pacific RII for the 2008-2010 re-run forecasts (N=509). Also shown for comparison is the skill of the operational version of the RII for those same forecasts. The numbers of RI cases for each RI threshold are also shown in orange.

4. **Future year 2 work**

The new Experimental Atlantic (Experimental_V2 version) and E. Pacific version of the RII will be re-derived using the updated SHIPS database that includes cases from the 2010 Hurricane Season. These new experimental versions will be run in parallel mode and their output made available to forecasters via a real-time link that has been established specifically for the testing of experimental RI products at CIRA during the upcoming 2011 Hurricane Season.

A parallel effort will also work toward 1) establishing a real-time feed of the operational NESDIS TPW product into the NHC, and 2) developing the stand along subroutines to create the IR principle components from the operational data feeds on the NCEP IBM. These efforts, if completed, would enable running of the experimental versions of the RII in a truly operational manner during the 2011 Hurricane Season. There remain many obstacles, mostly security related, at this time for establishing the TPW feed in task (1) to NHC and there is a considerable amount of coding required for completion of task (2). If these tasks cannot be completed in time the experimental RII will continue to run at CIRA in 2011 and tasks 1 & 2 will be completed in time for the 2012 hurricane season.

References:

Cione, J.J., and E.W. Uhlhorn, 2003: Sea Surface temperature variability in hurricanes: Implications with respect to intensity change. *Mon. Wea. Rev.*, **131**, 1783-1796.

Dunion, J.D., 2011: Re-writing the climatology of the tropical North Atlantic and Caribbean Sea atmosphere. *J. Climate*, **24**, 893-908.

Kaplan, J, M. DeMaria and J. A. Knaff, 2010: A revised tropical cyclone rapid intensification index for the Atlantic and eastern North Pacific basins, *Wea. Forecasting*, **25,** 220-241.

Knaff, J.A., 2008: Rapid tropical cyclone transitions to major huricane intensity: Structural evolution of infrared imagery. *Preprints 28th Conf. on Hurricanes and Tropical Meteorology*, Orlando, FL, Amer. Meteor. Soc.